

Published in final edited form as:

Nature. 2008 August 21; 454(7207): 1005–1008. doi:10.1038/nature07170.

The Pathogen Protein EspF_U Hijacks Actin Polymerization Using Mimicry and Multivalency

Nathan A. Sallee^{1,2}, Gonzalo M. Rivera³, John E. Dueber^{2,†}, Dan Vasilescu³, R. Dyche Mullins², Bruce J. Mayer³, and Wendell A. Lim²

¹Graduate Program in Chemistry and Chemical Biology, University of California, San Francisco, 600 – 16th Street, San Francisco, CA 94158.

²Department of Cellular and Molecular Pharmacology, University of California, San Francisco, 600 – 16th Street, San Francisco, CA 94158.

³Raymond and Beverly Sackler Laboratory of Genetics and Molecular Medicine, Department of Genetics and Developmental Biology and Center for Cell Analysis and Modeling (CCAM), University of Connecticut Health Center, Farmington, CT 06030.

Abstract

Enterohemorrhagic *E. coli* (EHEC) attaches to the intestine through actin pedestals that are formed when the bacterium injects the protein EspF_U into host cells¹. EspF_U potently activates the host WASP (Wiskott-Aldrich syndrome protein) family of actin-nucleating factors, which are normally activated by the GTPase Cdc42, among other signaling molecules. Apart from its N-terminal type III secretion signal, EspF_U consists of five and a half 47-amino-acid repeats. Here we find that a 17-residue motif within this EspF_U repeat is sufficient for interaction with N-WASP. Unlike most pathogen proteins that interface with the cytoskeletal machinery, this motif does not mimic natural upstream activators: instead of mimicking an activated state of Cdc42, EspF_U mimics an autoinhibitory element found within N-WASP. Thus EspF_U activates N-WASP by competitively disrupting the autoinhibited state. By mimicking an internal regulatory element and not the natural activator, EspF_U selectively activates only a precise subset of Cdc42-activated processes. Although one repeat is able to stimulate actin polymerization, we show that multiple-repeat fragments have dramatically increased potency. The activities of these EspF_U fragments correlate with their ability to coordinate activation of at least two N-WASP proteins. Thus this pathogen has used a simple autoinhibitory fragment as a component to build a highly effective actin polymerization machine.

Many pathogens target their host's cytoskeletal machinery to facilitate attachment, entry, or cell-to-cell spreading^{2, 3}. EHEC (O157:H7) causes severe gastrointestinal disease, and infection is dependent on attachment of the bacterium to intestinal epithelial cells via actin pedestals¹. Pedestal formation is mediated by the pathogenic protein EspF_U (also known as TccP)^{4, 5}, which is injected through a type III secretion system⁶ into host cells where it stimulates actin polymerization by activating host WASP proteins (Fig. 1a). WASPs are activators of the Arp2/3 complex, but under basal conditions this function is regulated by an autoinhibitory interaction between the GTPase-binding domain (GBD) and the "C" helix in the catalytic WCA region⁷. Normal activation of neuronal WASP (N-WASP) requires disruption of autoinhibition (Fig. 1b), involving coordinated action of multiple endogenous

Correspondence and requests for materials should be addressed to W.A.L. (lim@cmp.ucsf.edu).

[†]Present Address: Department of Synthetic Biology, California Institute of Quantitative Biomedical Research (QB3), University of California, Berkeley, 717 Potter Street, Berkeley, CA 94720.

Supplementary Information is linked to the online version of the paper at www.nature.com/nature.

activators, including Cdc42, the phospholipid PIP₂, and SH3-domain-containing proteins such as Nck^{8, 9} (Fig. 1c). EspF_U can independently activate N-WASP with a potency that is orders of magnitude higher than single endogenous activators⁸ (Fig. 1c,d, Fig. S1).

A common strategy exploited by pathogens in targeting host cell processes is to produce a protein that mimics an endogenous activator of that process^{6, 10, 11}. This mimic will generally be constitutively active compared to the endogenous protein, which shows regulated activity^{12, 13}. Among pathogens that target actin polymerization, there are examples of effector proteins that mimic the active states of N-WASP¹⁴ or N-WASP activators like Cdc42¹⁵. Previous studies have shown that EspF_U interacts with the GBD^{16, 17}, the regulatory domain in N-WASP that participates in autoinhibition and binds to activated Cdc42⁷. Thus, we set out to test the hypothesis that EspF_U may mimic an activated state of Cdc42.

EspF_U has a type III secretion signal followed by five and a half 47-amino-acid repeats (Fig. 1e) (a six-and-a-half-repeat isoform of EspF_U has also been reported⁵). The repeats are nearly identical and share little sequence homology with other proteins, except for the related EHEC protein EspF. EspF also activates N-WASP¹⁸ but does not participate in pedestal formation^{4, 19} (EspF contributes to the disruption of epithelial tight junctions).

We first mapped the minimal interacting fragments of both EspF_U and N-WASP using pulldown-binding assays. We found that the N-WASP GBD could bind to a single EspF_U repeat. We tested other truncations and found that the first 17 amino acids of each repeat constitute the minimal fragment with high-affinity for the GBD (Fig. 1f, Fig. S2). This sequence corresponds to a predicted α -helix²⁰ and it is repeated six times in the full-length protein. There are minor sequence differences among the six copies of this motif, but the repeats appear to be equivalent in binding and functional assays (data not shown).

The N-WASP GBD is a composite regulatory domain made up of two overlapping elements – a Cdc42-binding element and an autoinhibitory element that binds to the C helix⁷. Detailed mapping of the N-WASP side of the interaction showed that the C-terminal, autoinhibitory portion of the GBD interacts with EspF_U and the N-terminal, Cdc42-binding portion does not. The minimal EspF_U-binding fragment of N-WASP is residues 228–270 (Fig. 1f, Fig. S2), which form the core of the interaction with the C helix in the autoinhibited structure (Fig. 2a)⁷.

Since a small peptide from EspF_U interacts with the autoinhibitory portion of the GBD, it seemed unlikely that EspF_U was activating N-WASP by mimicking Cdc42. Instead, we postulated that this EspF_U fragment might be mimicking the C helix and disrupting N-WASP autoinhibition by competitively binding to the GBD. We found that EspF_U does indeed competitively disrupt the N-WASP GBD autoinhibitory interaction in a pulldown-binding assay (Fig. 2b). Sequence alignment of the C helix and the first 17 amino acids of the EspF_U repeat revealed sequence homology at three positions where hydrophobic amino acids are known to be critical for interaction with the GBD (Fig. 2a,c)²¹. We carried out a systematic alanine scan of both the N-WASP and EspF_U fragments and tested binding of the mutants to the GBD. The results showed that mutation of any of the conserved hydrophobic positions to alanine on either the C helix or the EspF_U fragment completely disrupted interaction with the GBD (Fig. 2c).

Previous work has shown that the isolated WASP GBD is only partially folded and unstable, but that fusion of the C helix to the GBD leads to a stably folded, helical structure that approximates the autoinhibited state⁷. We made a fusion of the GBD to the minimal 17-amino-acid interacting fragment from EspF_U found that this protein had very similar helical content and thermal stability to the GBD-C helix fusion (Fig. S3).

These results show that the N-terminal 17 amino acids of the EspF_U repeat are mimicking the C helix (an autoinhibitory element) and this motif competitively disrupts autoinhibition of WASPs (Fig. 2d). A similar sequence motif is present in EspF and likely activates N-WASP using the same mechanism. We found that one EspF_U repeat binds to the N-WASP GBD (amino acids 214–274) with a K_d of 18 nM (Fig. S4). This affinity is about 100-fold tighter than previously measured values for the corresponding WASP GBD-C helix interaction (*in trans*)⁷ and this higher affinity explains how an intermolecular interaction can competitively disrupt an intramolecular interaction. The C helix also contributes to N-WASP's interactions with actin monomers and the Arp2/3 complex²². We found that EspF_U can bind to these molecules as well (Fig. S4). In spite of this, EspF_U cannot stimulate actin polymerization without N-WASP (data not shown).

Utilization of a competitive autoinhibitory fragment represents a novel strategy for a pathogen to use in hijacking host cell signaling. One possible advantage of this strategy is increased specificity: a constitutively active signaling mimic will activate all downstream endogenous signaling pathways, whereas a mimic of a regulatory element should only activate a small subset. To test this idea we investigated whether EspF_U could activate the p21-activated kinases (PAKs) – another group of Cdc42-responsive proteins whose regulation is most closely related to WASPs'. Cdc42 activates PAKs by disrupting an autoinhibitory interaction (which is structurally homologous to that of WASP)²³. However, the PAK homolog of the WASP C helix lacks the consensus sequence of three conserved hydrophobic amino acids. EspF_U was unable to activate PAKs (Fig. 2e, Fig. S5), indicating specificity of EspF_U towards WASP family proteins (Fig. 2d). This more targeted activation may be advantageous for the pathogen, given the broad range of downstream effects mediated by WASP activators like Cdc42.

We also investigated the functional significance of this autoinhibitory mimic being repeated six times in one EspF_U molecule. We tested the relative abilities of different length EspF_U fragments to stimulate actin assembly using an *in vitro* pyrene-actin polymerization assay. One repeat from EspF_U can disrupt the N-WASP autoinhibitory interaction in a binding assay (Fig. S6), but has low ability to stimulate actin polymerization (comparable to a single endogenous activator) (Fig. 3a). A fragment of two repeats shows intermediate activity in the actin assay, but at least three repeats are necessary for high potency. Each additional repeat gives higher activity until full-length EspF_U (residues 80–337, lacking the secretion signal), which has a maximal activity at the same level as unregulated N-WASP (Fig. 3a, Fig. S7). To see if this trend continued, we made an EspF_U protein that has eight and a half repeats and found that it reaches the same maximal activity as the wildtype protein, but is even more potent at low concentrations (Fig 3a). At very high concentrations, EspF_U proteins had a partial inhibitory effect on actin polymerization (data not shown), likely due to EspF_U sequestering actin monomers and/or Arp2/3.

We constructed a minimized EspF_U protein in which six copies of the 17-residue C-helix mimic are separated by glycine-serine linkers. This construct was still able to stimulate actin polymerization (albeit with lower potency than wildtype EspF_U), showing that the C-terminal portion of each EspF_U repeat is not essential for activity (Fig. S8).

Next, we tested whether multiple repeats were also required in more complex assays of actin assembly – namely a reconstituted bead motility assay and an *in vivo* clustering assay. In the first assay, EspF_U fragments are chemically coupled to polystyrene beads and these beads are incubated with a mixture of actin and actin-regulatory proteins and examined by microscopy for the ability to stimulate actin assembly and motility²⁴. Beads coated with full-length EspF_U triggered formation of an F-actin shell that breaks symmetry and induces transient polarized bead movement (Fig. 3b). Beads coated with three EspF_U repeats showed similar behavior (albeit with a slightly more diffuse actin shell), while two-repeat beads formed shells

that were very diffuse, showed significantly reduced actin fluorescence, and disassembled within minutes. Beads coated with a single repeat showed minimal ability to polymerize actin (Fig. 3b). We varied the surface density of EspF_U protein on the beads and found that this had little effect on the relative activities of the different fragments (data not shown). In particular, one-repeat beads had weak activity, even at maximal density. This shows that a high local concentration of a single repeat has minimal effect – multiple repeats in the same polypeptide chain are required for potent activation of actin polymerization.

To test the ability of EspF_U fragments to form actin structures in cells, we used an antibody-induced clustering assay. Previous work has shown that N-WASP or N-WASP activators can form actin structures when clustered at the plasma membrane²⁵. In our assay, the EspF_U fragment is expressed as a fusion to the cytoplasmic tail of a transmembrane protein and then clustered using an antibody that recognizes the extracellular portion of the protein²⁶. Upon clustering of full-length EspF_U, we observed co-localization of N-WASP and bright actin foci to the clusters, showing that clustering of EspF_U is sufficient to trigger localized actin assembly (Fig. 3c, Fig. S9, S10). Furthermore, we tested three-, two- and one-repeat fragments and observed the same trend: three repeats showed similar activity to full-length, two repeats had intermediate activity and one repeat had lower activity (Fig. 3c). We used a computational image analysis tool (D. Vasilescu, unpublished) to detect and correlate antibody and actin clusters (Fig. S11). These quantitative results show that clustering of EspF_U fragments with more repeats causes formation of actin clusters with higher frequency and intensity (Fig. 3d).

The requirement of multiple repeats for activation of actin polymerization suggests that EspF_U needs to simultaneously bind and activate multiple N-WASP proteins to be highly active. To address this, we investigated the stoichiometry of the EspF_U – N-WASP complex using analytical ultracentrifugation (AUC). By AUC (data not shown) and binding assays (Fig. S12), we found that each repeat in an EspF_U fragment could simultaneously bind an isolated N-WASP GBD (for example, a three-repeat fragment bound to three GBDs). However, the model that EspF_U has high potency because it can activate multiple N-WASPs does not explain why a two-repeat fragment has lowered activity in our actin assays. We found a likely answer to this question through stoichiometric analyses of complexes of a two-repeat protein with a larger, autoinhibited N-WASP construct. This AUC data showed that while the two-repeat fragment can bind one N-WASP easily, binding of a second is less favorable (possibly due to steric effects) and only happens in large excess of N-WASP (Fig. S13). Larger fragments of EspF_U, on the other hand, readily formed complexes with two or more autoinhibited N-WASP proteins (Fig. S13). Taken with our activation data, this suggests that activity of EspF_U fragments correlates with their ability to coordinate the activation at least two N-WASP proteins (Fig. 3e). There are a number of other cases where oligomerization of WASPs or WASP activators leads to similarly increased activity – including the potent actin polymerization induced by GST-tagged N-WASP WCA²⁷ (presumably due to GST dimerization) and by oligomerized SNX9 in endocytosis²⁸.

We have shown here that the EHEC protein EspF_U has evolved a unique mechanism to potently and specifically activate N-WASP-mediated actin polymerization through a repeated autoinhibitory mimic. This co-opting of a small internal regulatory unit for activation of a target protein represents a novel pathogenic strategy. Furthermore, multiple repeated copies of this motif are essential for potent activity, apparently because a single EspF_U protein must coordinate simultaneous activation of multiple N-WASPs.

Methods Summary

EspF_U expression and purification

EspF_U fragments were amplified by PCR from EHEC genomic DNA (ATCC). All cloning and expression was done in *E. coli* BLR(DE3) strains lacking recombinase A.

Pyrene-actin polymerization assay

Arp2/3 was purified from bovine brain and actin was purified from rabbit muscle and pyrene-labeled, as previously described²⁹. Actin polymerization was monitored as an increase in pyrene-actin fluorescence. Raw fluorescence data were normalized to the lower and upper baselines of each curve. Relative activities of EspF_U fragments were determined through calculation of the time required to reach half-maximal fluorescence ($t_{1/2}$).

Bead motility assay

Actin and Arp2/3 were purified from *Acanthamoeba castellanii*, as previously described³⁰. EspF_U proteins were coupled to polystyrene beads and mixed with actin, Arp2/3, N-WASP, capping protein and profilin. The assay was adapted from a protocol developed by Orkun Akin & R. D. Mullins²⁴. Images were acquired with a Nikon TE300 Eclipse inverted epifluorescence microscope with constant imaging settings between experiments.

In vivo clustering experiments

NIH 3T3 fibroblasts were co-transfected with actin-GFP and the corresponding CD16/7 fusion construct. Cells were treated with clustering antibodies, as previously described²⁶. Fixed cells were imaged with an oil-immersion 60X NA 1.4 objective on a Zeiss LSM 510 Meta microscope. Imaging settings were constant between experiments, except for minor adjustments of detector gain to accommodate variation in expression level.

Quantitative detection of clusters was done with a computational tool developed by D. Vasilescu. Ten cell images from three independent experiments were quantified for each construct. Data were presented in two metrics: the percentage of antibody clusters that have associated actin clusters and the intensities of these associated actin clusters. The relative intensity value is the ratio of the sum of intensities of associated actin clusters to the sum of intensities of all antibody clusters.

Supplementary Material

Refer to Web version on PubMed Central for supplementary material.

References

1. Caron E, et al. Subversion of actin dynamics by EPEC and EHEC. *Curr. Opin. Microbiol* 2006;9:40–45. [PubMed: 16406772]
2. Gruenheid S, Finlay BB. Microbial pathogenesis and cytoskeletal function. *Nature* 2003;422:775–781. [PubMed: 12700772]
3. Rottner K, Lommel S, Wehland J, Stradal TE. Pathogen-induced actin filament rearrangement in infectious diseases. *J. Pathol* 2004;204:396–406. [PubMed: 15495265]
4. Campellone KG, Robbins D, Leong JM. EspF_U is a translocated EHEC effector that interacts with Tir and N-WASP and promotes Nck-independent actin assembly. *Dev. Cell* 2004;7:217–228. [PubMed: 15296718]
5. Garmendia J, et al. TccP is an enterohaemorrhagic *Escherichia coli* O157:H7 type III effector protein that couples Tir to the actin-cytoskeleton. *Cell. Microbiol* 2004;6:1167–1183. [PubMed: 15527496]

6. Galan JE, Wolf-Watz H. Protein delivery into eukaryotic cells by type III secretion machines. *Nature* 2006;444:567–573. [PubMed: 17136086]
7. Kim AS, Kakalis LT, Abdul-Manan N, Liu GA, Rosen MK. Autoinhibition and activation mechanisms of the Wiskott-Aldrich syndrome protein. *Nature* 2000;404:151–158. [PubMed: 10724160]
8. Prehoda KE, Scott JA, Mullins RD, Lim WA. Integration of multiple signals through cooperative regulation of the N-WASP-Arp2/3 complex. *Science* 2000;290:801–806. [PubMed: 11052943]
9. Rohatgi R, Nollau P, Ho HY, Kirschner MW, Mayer BJ. Nck and phosphatidylinositol 4,5-bisphosphate synergistically activate actin polymerization through the N-WASP-Arp2/3 pathway. *J. Biol. Chem* 2001;276:26448–26452. [PubMed: 11340081]
10. Mattoo S, Lee YM, Dixon JE. Interactions of bacterial effector proteins with host proteins. *Curr. Opin. Immunol* 2007;19:392–401. [PubMed: 17662586]
11. Stebbins CE. Structural insights into bacterial modulation of the host cytoskeleton. *Curr. Opin. Struct. Biol* 2004;14:731–740. [PubMed: 15582397]
12. Mukherjee S, Hao YH, Orth K. A newly discovered post-translational modification—the acetylation of serine and threonine residues. *Trends Biochem. Sci* 2007;32:210–216. [PubMed: 17412595]
13. Aktories K, Barbieri JT. Bacterial cytotoxins: targeting eukaryotic switches. *Nat. Rev. Microbiol* 2005;3:397–410. [PubMed: 15821726]
14. Zalevsky J, Grigorova I, Mullins RD. Activation of the Arp2/3 complex by the *Listeria acta* protein. Acta binds two actin monomers and three subunits of the Arp2/3 complex. *J. Biol. Chem* 2001;276:3468–3475. [PubMed: 11029465]
15. Alto NM, et al. Identification of a bacterial type III effector family with G protein mimicry functions. *Cell* 2006;124:133–145. [PubMed: 16413487]
16. Lommel S, Benesch S, Rohde M, Wehland J, Rottner K. Enterohaemorrhagic and enteropathogenic *Escherichia coli* use different mechanisms for actin pedestal formation that converge on N-WASP. *Cell. Microbiol* 2004;6:243–254. [PubMed: 14764108]
17. Garmendia J, Carlier MF, Egile C, Didry D, Frankel G. Characterization of TccP-mediated N-WASP activation during enterohaemorrhagic *Escherichia coli* infection. *Cell. Microbiol* 2006;8:1444–1455. [PubMed: 16922863]
18. Alto NM, et al. The type III effector EspF coordinates membrane trafficking by the spatiotemporal activation of two eukaryotic signaling pathways. *J. Cell Biol* 2007;178:1265–1278. [PubMed: 17893247]
19. McNamara BP, et al. Translocated EspF protein from enteropathogenic *Escherichia coli* disrupts host intestinal barrier function. *J. Clin. Invest* 2001;107:621–629. [PubMed: 11238563]
20. Rost B, Yachdav G, Liu J. The PredictProtein server. *Nucleic Acids Res* 2004;32:W321–W326. [PubMed: 15215403]
21. Panchal SC, Kaiser DA, Torres E, Pollard TD, Rosen MK. A conserved amphipathic helix in WASP/Scar proteins is essential for activation of Arp2/3 complex. *Nat. Struct. Biol* 2003;10:591–598. [PubMed: 12872157]
22. Marchand JB, Kaiser DA, Pollard TD, Higgs HN. Interaction of WASP/Scar proteins with actin and vertebrate Arp2/3 complex. *Nat. Cell Biol* 2001;3:76–82. [PubMed: 11146629]
23. Lei M, et al. Structure of PAK1 in an autoinhibited conformation reveals a multistage activation switch. *Cell* 2000;102:387–397. [PubMed: 10975528]
24. Akin O, Mullins RD. Capping protein increases the rate of actin-based motility by promoting filament nucleation by the Arp2/3 complex. *Cell* 2008;133:841–851. [PubMed: 18510928]
25. Castellano F, et al. Inducible recruitment of Cdc42 or WASP to a cell-surface receptor triggers actin polymerization and filopodium formation. *Curr. Biol* 1999;9:351–360. [PubMed: 10209117]
26. Rivera GM, Briceno CA, Takeshima F, Snapper SB, Mayer BJ. Inducible clustering of membrane-targeted SH3 domains of the adaptor protein Nck triggers localized actin polymerization. *Curr. Biol* 2004;14:11–22. [PubMed: 14711409]
27. Higgs HN, Pollard TD. Activation by Cdc42 and PIP(2) of Wiskott-Aldrich syndrome protein (WASP) stimulates actin nucleation by Arp2/3 complex. *J. Cell Biol* 2000;150:1311–1320. [PubMed: 10995437]

28. Yarar D, Waterman-Storer CM, Schmid SL. SNX9 couples actin assembly to phosphoinositide signals and is required for membrane remodeling during endocytosis. *Dev. Cell* 2007;13:43–56. [PubMed: 17609109]
29. Sallee NA, Yeh BJ, Lim WA. Engineering modular protein interaction switches by sequence overlap. *J. Am. Chem. Soc* 2007;129:4606–4611. [PubMed: 17381089]
30. Dayel MJ, Holleran EA, Mullins RD. Arp2/3 complex requires hydrolyzable ATP for nucleation of new actin filaments. *Proc. Natl. Acad. Sci. U. S. A* 2001;98:14871–14876. [PubMed: 11752435]

Acknowledgements

We thank O. Akin for reagents and assistance with the bead motility experiments; J. C. Anderson, A. Chau, R. Howard, M. Lohse, A. Remenyi & L. Weaver for assistance; and members of the Lim lab for discussion. This work was supported by grants from the NIH (NIGMS and Nanomedicine Development Centers, NIH Roadmap), the NSF and the Packard Foundation. G.M.R. was supported by the American Heart Association.

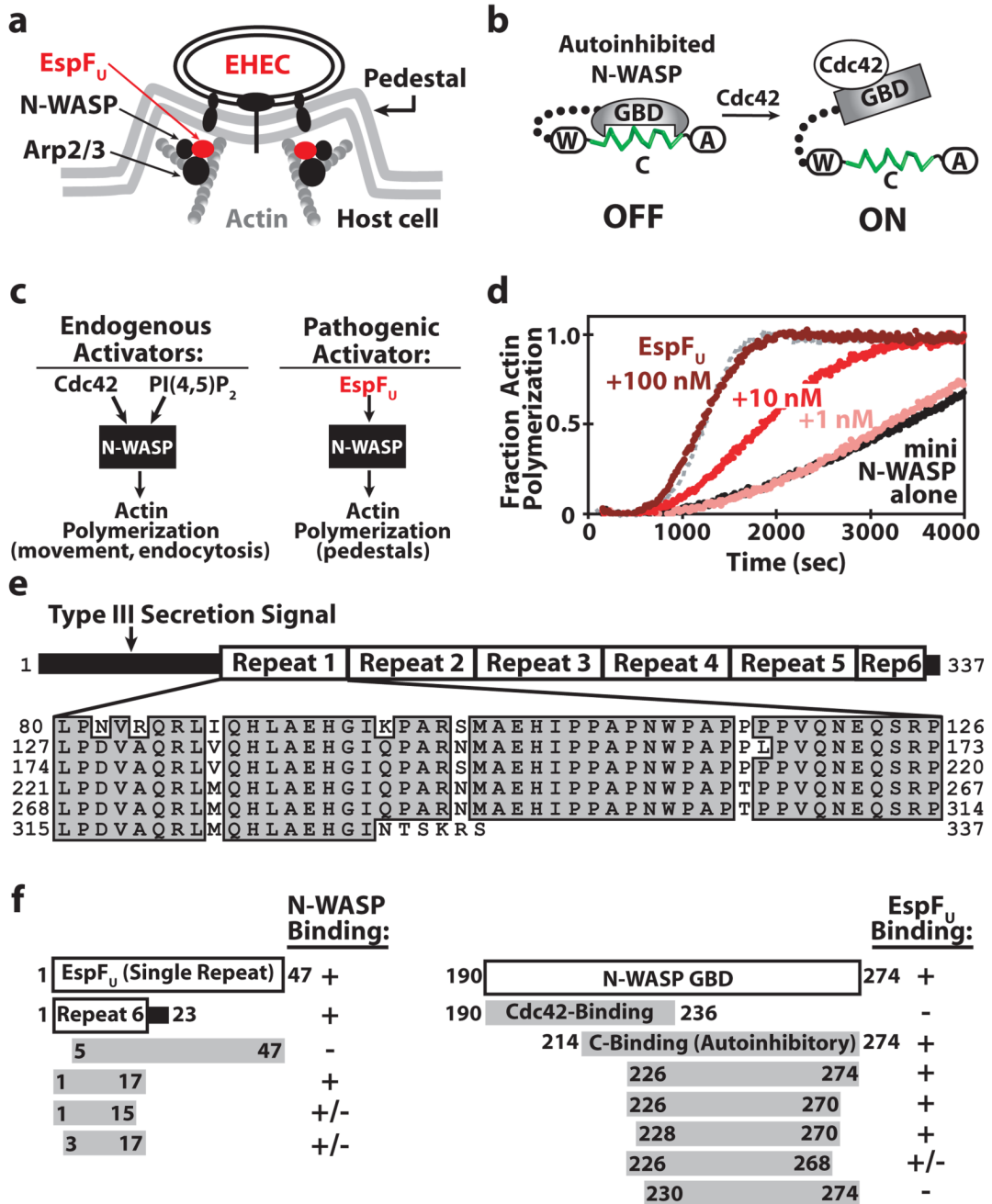


Figure 1. EspF_U is a potent activator of N-WASP

a, EspF_U is secreted from EHEC into a host cell where it stimulates actin polymerization through endogenous N-WASP and Arp2/3, leading to pedestal formation. **b**, N-WASP is basally autoinhibited, but can be activated by inputs like Cdc42. **c**, Multiple endogenous activators are necessary to potently activate N-WASP. EspF_U accomplishes this with a single input. **d**, EspF_U potently activates N-WASP in an *in vitro* pyrene-actin polymerization assay. Maximal rate (50 nM unregulated N-WASP WCA) shown in gray dotted line. All other reactions contain 50 nM mini N-WASP (B-GBD-linker-WCA). **e**, Sequence of EspF_U. **f**, Mapping minimal binding fragments of EspF_U and N-WASP with a glutathione S-transferase (GST) pulldown assay.

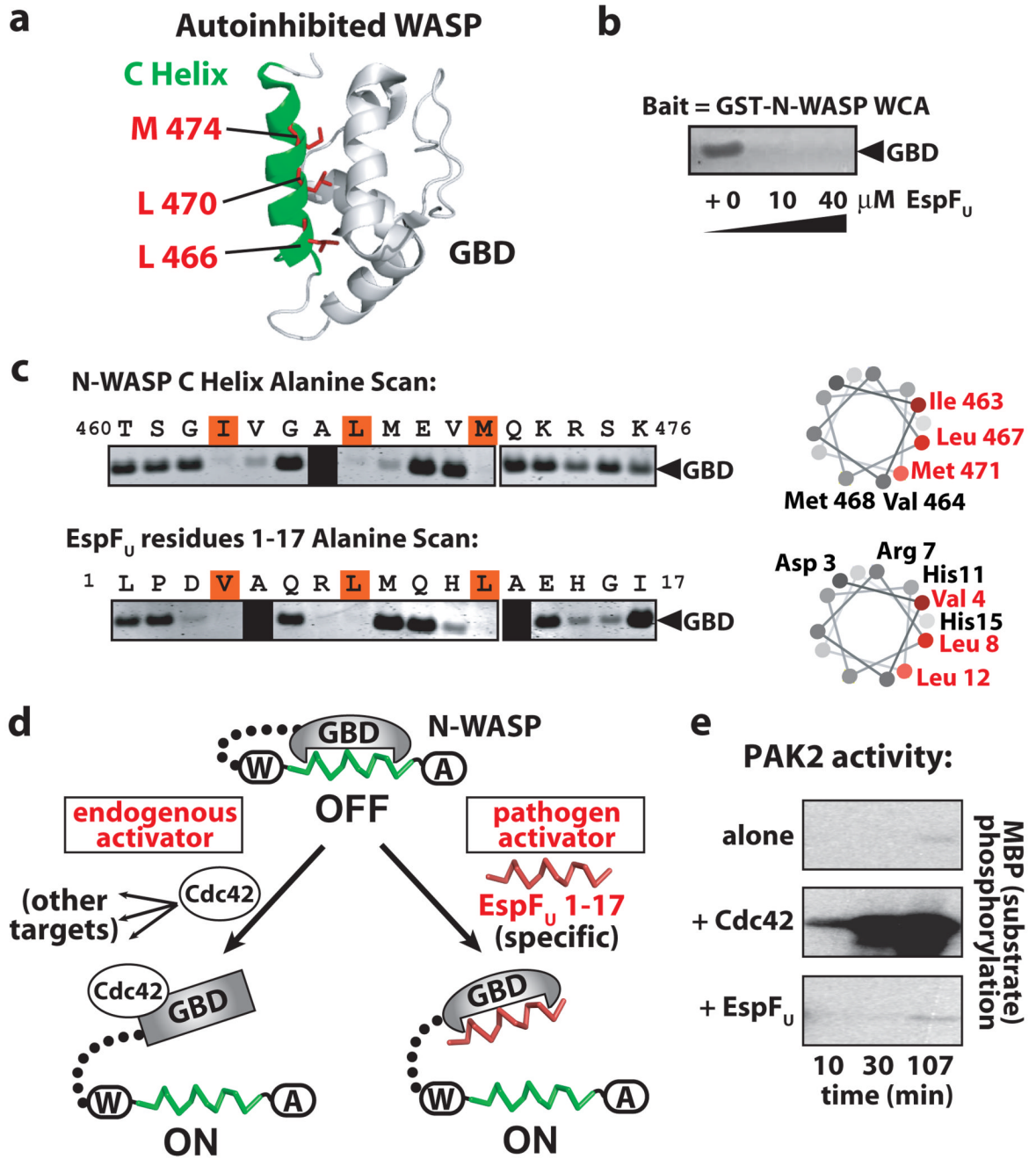


Figure 2. EspF_U mimics the N-WASP autoinhibitory C helix
a, Structure of autoinhibited fragment of WASP⁷, highlighting the C helix (green) and three critical side chains (red). **b**, EspF_U can competitively disrupt the N-WASP autoinhibitory interaction (*in trans*) in a GST-pulldown assay. **c**, Alanine scanning mutagenesis shows similar pattern of critical residues in N-WASP C helix and EspF_U (repeat 4, residues 1–17) (assayed by binding to GBD in a GST-pulldown assay). **d**, Model comparing N-WASP activation by Cdc42 and EspF_U. **e**, PAK kinase assay showing phosphorylation of myelin basic protein (MBP). PAK2 alone is autoinhibited – Cdc42 activates it, but EspF_U does not.

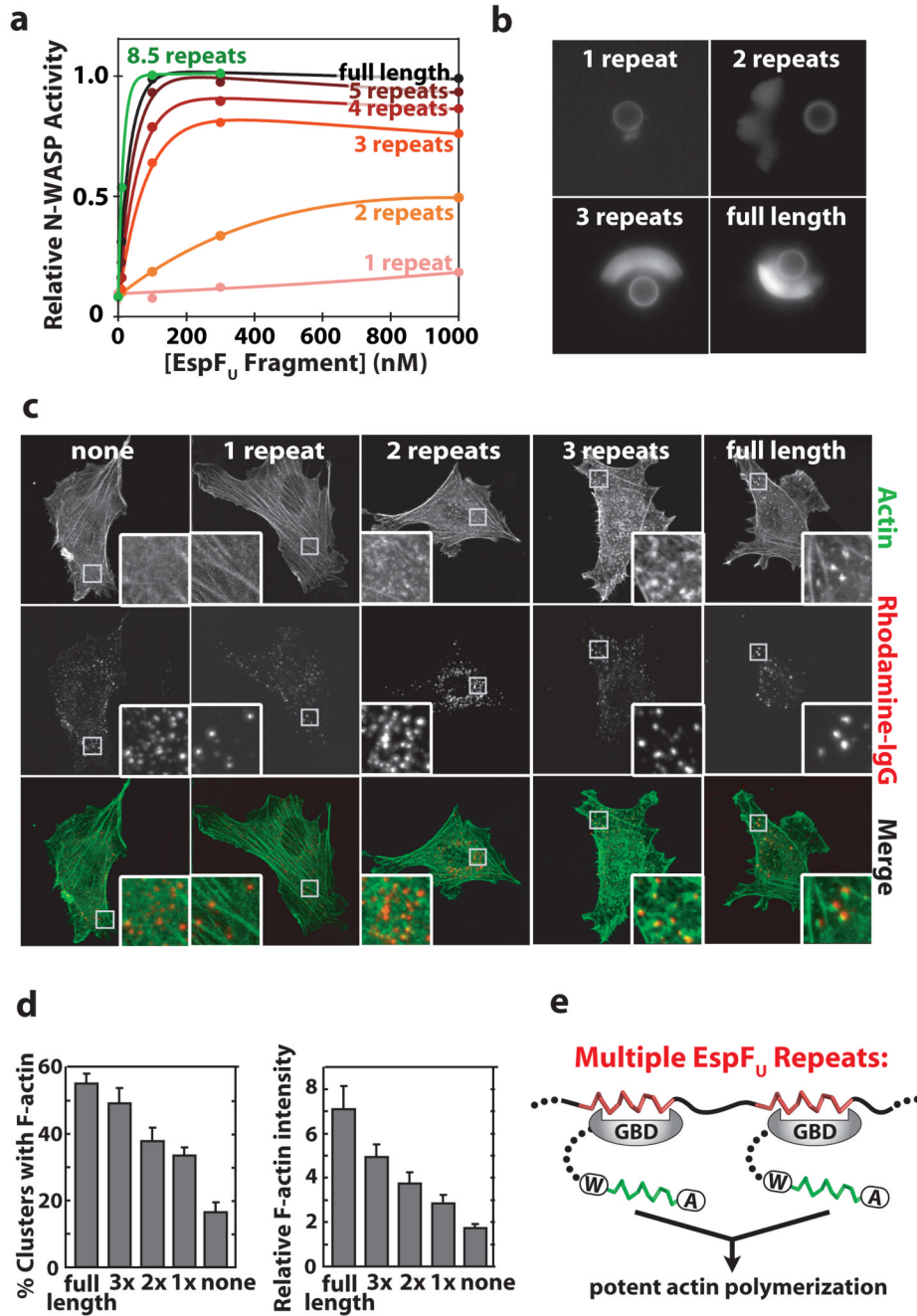


Figure 3. Multiple repeats of EspF_U are required for potent activation of actin polymerization
a, Activities of EspF_U fragments in a pyrene-actin polymerization assay. Data are fit to single exponential curves using MATLAB (MathWorks), with a small linear term subtracted to account for EspF_U sequestration of actin and/or Arp2/3. **b**, Visualization of fluorescently-labeled actin around beads coated with EspF_U fragments. Images were acquired four minutes after initiation. **c**, NIH 3T3 cells expressing GFP-actin and EspF_U fused to a transmembrane protein (CD16/7), which is clustered with a rhodamine-tagged antibody²⁶. Inset in each image is a portion of that cell (white box) shown at higher magnification. **d**, Results from quantification of clustered cells, shown in two metrics. Bars represent mean \pm s.e.m. of 10 cell

images. **e**, Activity correlates with ability of EspF_U fragments to bind at least two N-WASP proteins simultaneously.